

Robust adaptive sliding mode control of a bidirectional DC-DC converter feeding a resistive and CPL based on PSO

Julius Derghe Cham¹, Francis Lénine Djanna Koffi¹, Alexandre Teplaira Boum², Ambe Harrison³

¹Technology and Applied Sciences Laboratory (LATS), University of Douala, Douala, Cameroon

²Department of Electrical and Electronics Engineering, ENSET, University of Douala, Douala, Cameroon

³Department of Electrical and Electronics Engineering, College of Technology, University of Buea, Buea, Cameroon

Article Info

Article history:

Received May 23, 2024

Revised Aug 20, 2024

Accepted Aug 29, 2024

Keywords:

Bidirectional half-bridge

DC-DC converter

Constant power load

Particle swarm optimization

Robust adaptive controller

Robust controller

ABSTRACT

A DC-DC converter functioning in bidirectional (two-way) mode is a crucial component of direct current (DC) microgrids since it allows electricity to flow in both directions. However, because of load changes and other factors, the DC-bus voltage might become unstable. This research proposes a robust adaptive controller for a half-bridge two-way DC-DC converter founded on particle swarm optimization (PSO). Using a DC-DC half-bridge bidirectional converter, the effectiveness of various conventional and proposed control techniques is investigated. In comparison to a conventional sliding mode controller (CSMC), it is found that a PSO-based sliding mode control with an adaptive law is the optimal control approach for a bidirectional half-bridge DC-DC converter. This is because minimal steady-state error and the shortest rising and settling times are guaranteed. The benefits of robustness, chattering reduction, and simple design are combined in the suggested controller, which is especially beneficial when dealing with load and input voltage changes. The controller ensures robustness and stability in the face of parameter changes. Numerical simulations conducted in a MATLAB-Simulink environment on a DC-DC half-bridge converter operating in bidirectional mode show the controller's improved performance over its existing counterpart.

This is an open access article under the [CC BY-SA](#) license.



Corresponding Author:

Julius Derghe Cham

Technology and Applied Sciences Laboratory (LATS), University of Douala

P.O. Box, 7236 Douala, Cameroon

Email: julius.cham@yahoo.com

1. INTRODUCTION

Since they make it possible to employ renewable energy sources like wind, sun, and fuel, direct current (DC) microgrid installation, control, and exploitation have garnered increasing attention in the world. In addition, DC microgrids have several advantages over alternating current (AC) grids, including phase and frequency management, minimal conversion times, an easy-to-manage control structure, and the absence of reactive power compensation [1], [2]. A possible alternative for energy supply is DC microgrids, which are known for their excellent reliability and storage capacity [3], [4]. DC microgrids have many useful features, but they still have some drawbacks that need to be addressed, like constant power load (CPL) and pulsed power load (PPL) [5], [6]. The tendency of power electronic loads to consume constant power when closely regulated leads to negative incremental impedance characteristics, which lower the damping coefficients and create instability in the DC bus voltage [7]. The pulsed power load, which has a tendency to draw a large quantity of power in a brief length of time, is another problem with DC microgrids. Pulsed power load behavior is commonly observed on microgrids, such as those found in electric vehicles, ships, and airplanes. A system becomes unstable when a microgrid is moved far from a fixed operational point by a pulsed power load [5], [6].

Additionally, the nonlinear behavior of DC microgrids with CPL poses significant challenges to the application of linear control in an effort to regulate the system [8]. The primary components of DC microgrids that serve as interfaces between microgrids and energy sources or between two microgrids with varying bus voltages are two-way DC-DC converters [5]. Furthermore, power can flow in two directions with bidirectional DC-DC converters; nevertheless, there are concerns regarding their regulation inside the DC microgrid. Many researchers have developed linear or nonlinear control algorithms in the literature to solve some of these issues with DC microgrids that are fed by or receive power from DC power converters. A nonlinear double-integral backstepping sliding mode controller was extensively studied and utilized to stabilize the DC bus voltage of a DC-DC converter connected to a CPL [9]. The boost converter that feeds CPLs with minimal steady-state tracking error and quick transient reactions ensures DC-bus voltage stability even in the face of significant disturbances, according to the controller. In order to increase the DC bus voltage stability in a renewable energy-based DC microgrid, a two-way DC-DC converter is controlled by a proportional integral (PI) controller, which is presented in [10]. However, in the event of parameter fluctuations, a PI controller is not robust [11]. A new control approach for DC microgrids feeding a steady power load was developed by the authors in [7]. In addition to stabilizing the system as a whole, the buck converter was adjusted to ignore the impacts of outside uncertainties and disturbances. A buck converter providing a constant power load was suggested to have a strong nonsingular terminal sliding mode control in [1]. They looked into how to stabilize the bus voltage in a DC microgrid (MG) that supplies a CPL. In their study, they use a nonsingular terminal robust sliding mode controller to stabilize the main DC bus's output voltage. This controller eliminates the singularity issue that happens with traditional terminal sliding mode controllers. While two-way DC-DC converters feeding CPLs have been the subject of a few studies, one-directional DC-DC converters have received the majority of proposed works' attention.

A resilient sliding mode controller was suggested by the authors in [12] for a two-way DC-DC converter that interfaces with a storage unit in a DC microgrid that is dominated by CPLs. The suggested controller guarantees tight restrictions on DC bus voltage regulation. The writers of [5] and [13] provide an overview of two-way DC-DC converter advanced control techniques in DC microgrids and enumerate the best-advanced controllers for these types of converters. The review discussed a number of control strategies, each with pros and cons, including model predictive control, backstepping control, sliding mode control, passivity-based control, observer/estimation-based techniques, and intelligent control. A two-way DC-DC converter with a dynamic CPL was constructed with sliding mode control (SMC) in [2]. In comparison to the conventional PI controller and integral proportional integral derivative (IPID) controller, the suggested controller turned out to be more reliable. A continuous-time model predictive control of CPL stability in DC microgrids was designed by Alidrisi *et al.* [14]. Their simulation findings show that they performed well with regard to transient responsiveness, stability, and optimal tracking. Model predictive control (MPC) does have a problem with a large computational burden. Moreover, the whole plant model was needed for the system design, which might not always be available [5]. Because of its unit properties, which include enhanced dynamics and robustness for non-linear systems, the SMC stands out as a popular control approach, as described in the literature mentioned above. However, when the controller's gains are fixed, SMC experiences chattering problems and performs moderately in the presence of significant disturbances.

In an effort to lessen the chattering effect, its border layer jeopardizes tracking robustness and performance [15]. While the second-order SMC provides significant solutions for high-frequency chattering, the control system must perform numerical differentiation, which is not always a reliable procedure [16]. Kaplan and Bodur [17] proposed an SMC with a super-twisting algorithm for a step-down converter with CPL. Previous works have focused on using different techniques of optimization to ameliorate the performance of the SMC in DC-DC power converters. Among the methods for optimization are particle swarm optimization, genetic algorithms, and honey bee optimization algorithms [18], [19]. Although the particle swarm optimization (PSO) algorithm has demonstrated its worth as an optimization tool in several DC-DC power converters, its application is limited to half-bridge DC-DC converters operating in bidirectional modes with adaptive sliding mode control (ASMC) [20], [21].

This paper proposes a PSO for bidirectional DC-DC converter feeding resistance and CPL based on ASMC management with a modified sliding surface. By enabling the output voltage to remain constant at the targeted CPL power values, the suggested controller will ensure robustness and stability for the DC microgrid. Numerical simulation is used to implement the suggested controller in a MATLAB-Simulink context. The following are this paper's main contributions:

- To control the bus voltage in a half-bridge two-way DC-DC converter used in DC microgrid applications, a sliding mode controller with an adaptive law enhanced by particle swarm optimization (ASMCPSO) was proposed.
- It has been demonstrated that sliding mode control exists and is stable.

- Using numerical simulation in a MATLAB-Simulink environment, the controller's performance has been verified.
- The controller's robustness has been demonstrated under wide variations in source voltage, CPL power, and reference voltage in buck as well as boost modes of operation.

This paper continues as follows for the remainder of: i) The bidirectional DC-DC converter topology under consideration, along with its mathematical modeling, is provided in section 2; ii) The design of the suggested controller and the SMC are covered in section 3; iii) The proposed controller and the conventional sliding mode controller's simulation results are explained and contrasted in section 4; and iv) This paper concludes with a discussion of potential future directions in section 5.

2. METHODOLOGY

2.1. Description of the adopted methodology

In order to design an ideal control solution for a two-way DC-DC converter, this research takes a thorough and methodical approach. Figure 1 shows block diagram, which graphically depicts the methodological structure, and provides a clear and succinct summary of the whole procedure. Using numerical simulations and implementations in the environment of MATLAB/Simulink, we verify the stability and efficacy of the suggested control systems. We can model, analyze, and optimize complicated control systems with this simulation platform's flexible and potent toolkit, which enables us to thoroughly assess the effectiveness of our suggested solutions in a range of operational scenarios. The procedure starts with a thorough mathematical modeling of the adopted converter that takes into consideration its two different operating modes, boost, and buck. This modeling stage is essential because it establishes the framework for comprehending the behavior of the dynamic system and pinpointing the crucial variables that affect its functionality. We design the controllers for each mode of operation after the modeling stage. We painstakingly designed these controllers to address specific issues related to the converter's nonlinear dynamics. The next step after design is optimization when sophisticated methods like particle swarm optimization are used to adjust the controller parameters for the best results. Ultimately, the regulated system is put into practice within the environment of MATLAB/Simulink through extensive testing in a variety of scenarios. These tests enable us to fully examine the system's capabilities by varying the source voltage, CPL, and the desired output voltage.

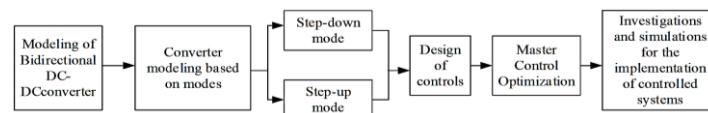


Figure 1. A thorough explanation of the research methods

2.2. Description of a DC microgrid

Research is being done on a two-way DC-DC converter, which is one of the key components of a DC microgrid that supplies CPLs. The basic design of a DC microgrid that supplies both DC and alternating current (AC) loads is shown in Figure 2. In the meantime, Figure 3 shows the analogous circuit of a half-bridge two-way DC-DC converter that can function in both boost and buck modes when fed CPL. A battery or storage unit, a two-way DC-DC converter that connects the grid and the battery, and a DC microgrid make up the system. The objective is to have the two-way DC-DC converter run in both boost and buck modes while maintaining a steady DC bus voltage. The battery absorbs and stores excess power from the distributed power source. The storage unit discharges to keep the DC microgrid's power balance when the grid's electricity is insufficient [2].

2.3. Modelling of bidirectional DC-DC converter

References [12] provide the structure of the two-way DC-DC converter supplying the CPLs that need to be modeled and managed. Figure 3 illustrates the equivalent circuit schematic of the converter based on the two modes of operation: Figure 3(a) for buck mode and Figure 3(b) for boost mode, respectively. The equivalent circuit of the converter used for charging and discharging the battery is presented in Figure 3 because the switches are complementary, meaning that when one is on, the other is off, and vice versa [12]. As a result, the control input d is designed as $d \in \{0,1\}$ when it is on and off, respectively. In this system, the converter lowers the DC bus voltage to charge the battery and increases the battery voltage to supply the loads connected to the DC bus. A resistance linked in parallel to a CPL represents the load in each mode. Buck mode as in (1) and boost mode as in (2), which can be found in [22], provide the average mathematical model of the circuit for each mode of operation when source internal resistances are disregarded.

$$\begin{cases} L \frac{dI_L}{dt} = dV_{in} - V_{C_2} \\ C_2 \frac{dV_{C_2}}{dt} = I_L - \frac{V_{C_2}}{R} - \frac{P_L}{V_{C_2}} \end{cases} \quad (1)$$

$$\begin{cases} L \frac{dI_L}{dt} = -(1-d)V_{C_1} - V_{Bat} \\ C_1 \frac{dV_{C_1}}{dt} = (1-d)I_L - \frac{V_{C_1}}{R} - \frac{P_L}{V_{C_1}} \end{cases} \quad (2)$$

Figure 2 shows V_{in} is the voltage from the DC microgrid supplying the converter, I_L denotes the current in the inductor, V_{C_1} and V_{C_2} are the voltages across the capacitors C_1 and C_2 respectively of the converter operating in step-up and step-down modes. R stands for the resistive load and P_L represents the steady or constant power load on the low and high voltage sides. The voltage across the capacitor is identical to the output voltage in each mode of operation.

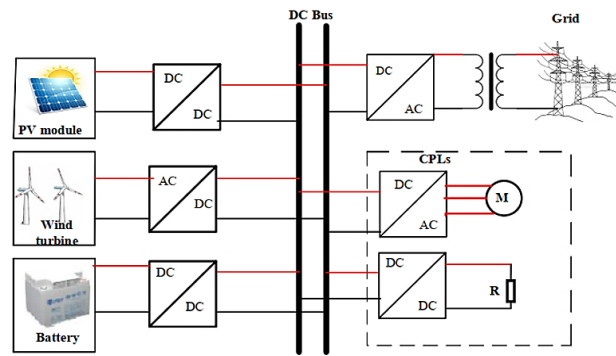


Figure 2. Typical DC microgrid system architecture

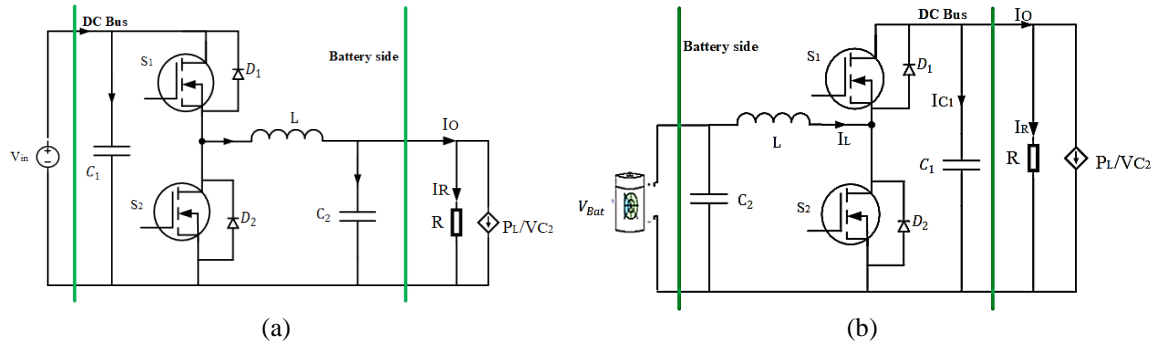


Figure 3. Equivalent circuit of two-way DC-DC converter: (a) buck mode and (b) boost mode

2.4. Constant power load

Through the half-bridge, two-way DC-DC converter, the DC bus is directly connected to the load in the DC microgrid, with the power taken by the load being constant, which is considered a CPL as found in [22]. It is perceived that when the power drawn by the load is constant, the voltage increases while the current reduces, which leads to nonlinear behavior and necessitates a non-linear controller. $I_{PL} = \frac{P_L}{V_{C_2}}$ or $I_{PL} = \frac{P_L}{V_{C_1}}$ depending of the mode of operation.

3. CONTROLLERS DESIGN

3.1. Sliding mode controller design for charging (buck) mode of operation

The generic SMC law, as stated in reference [22] and given in (3), is provided by adopting a switching function appropriate for this system that guarantees reachability and the presence of a sliding mode controller.

$$d = \frac{1}{2}(1 + \text{Sign}(S)) = f(x) = \begin{cases} 1, & \text{if } S > 0 \\ 0, & \text{if } S < 0 \end{cases} \quad (3)$$

Adopting a sliding surface from [21] given by (4).

$$S_{buck} = K_1 x_1 + x_2 \quad (4)$$

Where K_1 is the gain of the SMC. Considering V_{C_2} as the actual output voltage and V_{ref} as the desired output voltage, the corresponding state variables x_1 and x_2 may be expressed as (5).

$$x_1 = V_{ref} - V_{C_2}, x_2 = \frac{dx_1}{dt} = -\frac{dV_{C_2}}{dt} = -\frac{I_{C_2}}{C_2} \quad (5)$$

The time derivative of (4) may be given by $\dot{S} = K_1 \dot{x}_1 + \dot{x}_2$ with (6). Substituting (6) into (7), we obtain (8).

$$x_2 = \dot{x}_1 = \frac{dV_{in-V_{C_2}}}{L} \text{ but } x_1 = I_L = \int \frac{dV_{in-V_{C_2}}}{L} dt \quad (6)$$

$$x_2 = -\frac{I_L}{C_2} + \frac{V_{C_2}}{RC_2} + \frac{P_L}{V_{C_2}C_2} \quad (7)$$

$$x_2 = -\frac{1}{C_2} \left(\int \frac{dV_{in-V_{C_2}}}{L} dt \right) + \frac{V_{C_2}}{RC_2} + \frac{P_L}{V_{C_2}C_2} \quad (8)$$

Deriving (8), we get (9).

$$\dot{x}_2 = \frac{V_{C_2}}{LC_2} - d \frac{V_{in}}{LC_2} + \frac{I_{C_2}}{RC_2^2} - \frac{P_L}{V_{C_2}^2 C_2^2} I_{C_2} \quad (9)$$

The equivalent control law is obtained by solving $\dot{S} = 0$, this brings us to (10) and (11).

$$d_{eq} = \frac{L}{V_{in}} \left[-K_1 + \frac{1}{RC_2} - \frac{P_L}{C_2 V_{C_2}^2} \right] I_{C_2} + \frac{V_{C_2}}{V_{in}} \quad (10)$$

But, as in (10), with $d_n = \text{Sign}(S)$

$$d = d_{eq} + d_n \quad (11)$$

3.2. ASMC design for charging mode of operation.

The adaptive sliding surface law is chosen as found in [20] by (12).

$$M = S + \gamma \tanh(S) \int_0^t S dt \quad (12)$$

$\dot{M} = \dot{S} + \gamma S$ as being the derivative of the modified sliding surface as further defined in (13) and by substituting (9) in (13) brings us to (14).

$$\dot{M} = K_1 \dot{x}_1 + K_2 \dot{x}_2 + \gamma K_1 x_1 + \gamma x_2 \quad (13)$$

$$\dot{M} = K_1 x_2 + \frac{V_{C_2}}{LC_2} - d \frac{V_{in}}{LC_2} + \frac{x_2}{RC_2} + \frac{P_L x_2}{V_{C_2}^2 C_2} + \gamma K_1 x_1 + \gamma x_2 \quad (14)$$

By solving $\dot{M} = 0$ to obtain the equivalent control given in (15).

$$d_{eq} = \frac{LC_2}{V_{in}} \left[\left(K_1 - \frac{1}{RC_2} + \frac{P_L}{V_{C_2}^2 C_2} + \gamma \right) x_2 + \frac{V_{C_2}}{LC_2} + \gamma K_1 x_1 \right] \quad (15)$$

The (16) provides the discontinuous portion of the suggested sliding mode control law.

$$d_n = K_2 \tanh(M) \quad (16)$$

However, $\gamma = \frac{I_o}{V_{C_2}C_2}$; but $I_o = I_{P_L} + I_R$, in order to minimize chattering, as inspired by reference [22] the control law is selected as (17).

$$d = d_{eq} + K_3 \tan(S) \quad (17)$$

Then the adaptive control law becomes (15) and (18).

$$d = d_{eq} + K_2 \tanh(M) \quad (18)$$

To ensure conditions on the control law which will move the system states to the sliding manifold such that $M=0$, a candidate Lyapunov function μ is chosen as given in [23] and defined by (19).

$$\mu = \frac{1}{2} M^2 \quad (19)$$

The derivative of the above Lyapunov function with time can be calculated and is given by (20) that is $\dot{\mu} < 0$.

$$\dot{\mu} = M \dot{M} \quad (20)$$

The (14) and (18) are replaced in (20) to guarantee the system's stability and the attractiveness of M , which brings us to (21).

$$\dot{\mu} = M \left(0 - \frac{K_2 V_{in}}{LC_2} \tanh(S) \right) = \frac{K_2 V_{in}}{LC_2} \tanh(S) < 0 \text{ with } M > 0, \text{ where } K_2 > 0 \quad (21)$$

This condition can be verified by designing the nonlinear control scheme as $d_n = K_2 \tanh(S)$, with $\dot{\mu}$ being the derivative of μ respect to time, which must be negatively definite. Hence, the adaptive controller guarantees convergence and the stability of the system, according to Lyapunov.

3.3. SMC design for discharging (boost) mode of operation

Considering V_{C_1} represents the actual voltage at the output and V_{ref} the desired voltage at the output of the converter operating in boost mode, the corresponding state variables x_1 and x_2 may be expressed as (22).

$$x_1 = V_{ref} - V_{C_1}, x_2 = \frac{dx_1}{dt} = -\frac{dV_{C_1}}{dt} = -\frac{I_{C_1}}{C_1} \quad (22)$$

Selecting a sliding surface of (23).

$$S_{boost} = k_1 x_1 + x_2 \quad (23)$$

From (2), we found (24).

$$I_L = \int \frac{dV_{in} - V_{C_2}}{L} dt \quad (24)$$

$$\text{With } \bar{d} = 1 - d$$

The derivative of (22) is given in (25).

$$\text{But } \dot{x}_2 = \frac{dV_{C_1}}{LC_1} - \frac{V_{in}}{LC_1} + \frac{P_L x_2}{V_{C_1}^2 C_1} - \frac{x_2}{RC_1} \quad (25)$$

The derivative of the sliding surface is stated in (26)

$$\dot{S} = k_1 \dot{x}_1 + \dot{x}_2 \quad (26)$$

The equivalent control is obtained by solving $\dot{S} = 0$ which is given in (27).

$$d_{eq} = \frac{LC_1 \left[k_1 - \frac{1}{RC_1} + \frac{P_L}{V_{C_1}^2 C_1} \right] x_2 - V_{in} + V_{C_1}}{V_{C_1}} \quad (27)$$

The (28) gives the duty ratio,

$$0 < d = \frac{V_c}{V_{ramp}} < 1 \quad (28)$$

Comparing (27) and (28), the control signal becomes (29), with $V_{ramp} = V_{C_1}$.

$$V_c = LC_1 \left[k_1 - \frac{1}{RC_1} + \frac{P_L}{V_{C_1}^2 C_1} \right] x_2 - V_{in} + V_{C_1} \quad (29)$$

3.4. ASMC design for discharging mode of operation

In the boost mode of operation, a proportional-integral (PI) type function of the sliding surface is adopted from reference [24] and defined as (30).

$$M = S + \rho \tanh(S) \int_0^t |S| dt \quad (30)$$

Where H is the function of sliding function, ‘tanh’ represents a smooth hyperbolic tangent function, and $\rho > 0$ is a scalar. The existence of sliding modes is elaborated in reference [24] as well as more information on the adaptive control law. The ASMC of the converter operating in charging mode is obtained by solving $\dot{M}=0$. The derivative of (30) is defined in (31)

$$\dot{M} = K_1 \dot{x}_1 + K_2 \dot{x}_2 + \rho K_1 x_1 + \rho K_2 x_2 = 0 \quad (31)$$

The control law becomes (32).

$$d_{eq} = \frac{LC_1}{V_{C_1}} \left[\left(k_1 - \frac{1}{RC_1} + \frac{P_L}{V_{C_1}^2 C_1} + \rho \right) x_2 + k_1 \rho x_1 \right] - V_{in} + 1 \quad (32)$$

The load can be estimated as $R = \frac{V_{C_1}}{I_R}$ and the parameter ρ can be tuned according to the load with $\rho = \frac{I_R}{V_{C_1} C_1}$ making the sliding mode controller to become adaptive to load variation which can further be seen in [24].

3.5. Optimization of the ASMC gains

The suggested control law depends on certain control parameters, particularly and, as shown in (10) and (15). Therefore, these characteristics should be crucial to the converter's correct and optimal performance under the controller's coordination. It is crucial that these parameters be designed as optimally as possible. This paper recommends an offline modification utilizing particle swarm optimization to optimally identify these values. One popular stochastic optimization approach is PSO [19]. It is a member of the metaheuristics class of optimization. PSO has proven to be an effective optimization technique and has been used in many engineering and control system applications [21], [25]. As a result, PSO is used to tune and change the gains until the ideal time response performance is reached.

4. RESULTS AND DISCUSSION

Within the MATLAB-Simulink environment, a half-bridge, two-way DC-DC converter simulation model is constructed. To demonstrate the advantages of the suggested controller over the current controller, the charging and discharging modes of the converter and the impact of the control techniques are examined. The parameters of the bidirectional half-bridge DC-DC converter and the control techniques are presented in Tables 1-3, respectively [26], [27]. The input voltage, power absorbed, and reference voltage are all adjusted, in order, to evaluate how robustly the various control techniques hold up.

The reference is set to 24 volts, and the simulation lasts for 0.1 seconds. The converter is simulated using both the suggested controller and the classical sliding-mode controller. The results are shown in Figure 4. It is clear that both controllers keep the output voltage consistent with the reference voltage, although the recommended controller performs faster than the conventional controller. Figures 3(a) and 3(b) demonstrate how much faster the recommended controller is than the traditional one with the converter operating in buck mode.

Table 1. Half-bridge two-way DC-DC converter simulation parameters

| Parameters | Symbol | Value |
|---------------------|-----------|-------------|
| Input voltage | V_{in} | 48 V |
| Reference voltage | V_{C_2} | 24 V |
| Inductance | L | 100 μ H |
| Capacitance | C_1 | 5 mF |
| Capacitance | C_2 | 5 mF |
| Switching frequency | F_s | 20 KHz |

Table 2. Design parameters of various control strategies of buck mode

| CSMC | ASMCP SO |
|--------------|------------------|
| $k_1 = 2500$ | $K_1 = 5.2478e3$ |
| $k_2 = 5000$ | $K_2 = 1.7724e4$ |

Table 3. Design parameters of various control strategies of boost mode

| CSMC | ASMCP SO |
|--------------|-------------------------------|
| $k_1 = 3500$ | $K_1 = 5.484e3, 3.289e + 03$ |
| $k_2 = 1000$ | $K_2 = 2.3095e4, 5.318e + 03$ |

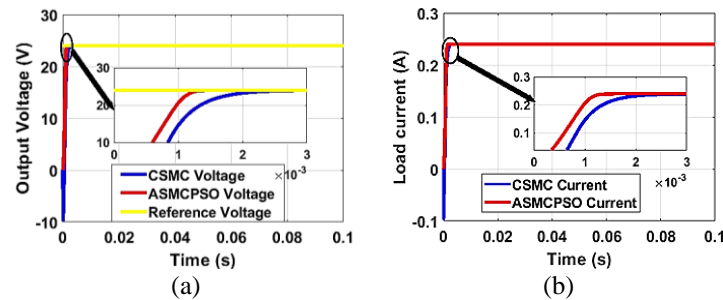


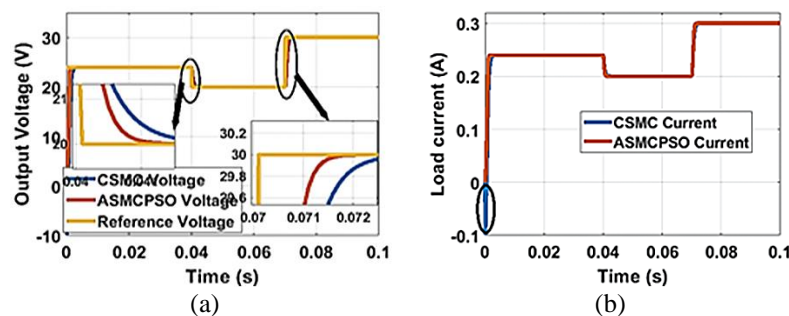
Figure 3. Comparing simulation results of the proposed controller with its conventional counterpart: (a) output voltage and (b) load current

4.1. Robustness tests by simulation

A comparative investigation of the performance of non-linear controllers on a two-way DC-DC converter is used for verification. This is achieved by testing the controllers' robustness against fluctuations in parameters. The CSMC and the recommended controller (ASMCP SO), are the controllers under investigation.

4.1.1. Variation of reference in buck mode (1st scenario)

In the first scenario, the reference voltage is changed step-by-step from 24 to 20 volts and from 20 to 30 volts at $t=0.04$ and $t=0.07$ seconds, respectively, while the power and input voltage remain fixed. The converter is controlled by CSMC and ASMPSO; Figure 4 displays the load current and output voltage data. As can be observed, every control structure performs noticeably well in following the reference voltage. However, from Figure 4(a), it is evident that the suggested controller responds more quickly to changes in the reference voltage. Voltage fluctuations cause the control structures to respond differently; however, the suggested controller showed the fastest response time in returning the output voltage of the DC-DC converter to its respective reference values. In comparison to the alternative controller, the suggested controller thus attains the maximum control tracking accuracy.

Figure 4. Comparing simulation results of the proposed controller with its conventional counterpart (1st scenario): (a) output voltage and (b) load current

4.1.2. Variation of absorbed power in buck mode (2nd scenario)

In the second scenario, the system is disrupted when the power suddenly changes from one value to another. Power supplies for power electronics, or DC-DC converters, typically need to react as fast as possible to power fluctuations in the load. The load admits a sudden change from 10 w to 5 w at $t=0.03$ seconds and from 5 w to 20 w at $t=0.07$ seconds, respectively. Figure 5 displays the step changes in the output power, and the simulation results for the different control methods are shown in Figures 6(a) and 6(b). The figures show that all control systems perform as the load is changed, with the ASMCP SO outperforming the conventional controller as it is capable of removing the negative current as indicated in Figure 4(b).

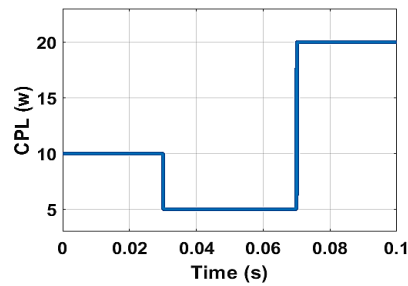


Figure 5. Step changes in the output power of the converter operating in buck mode

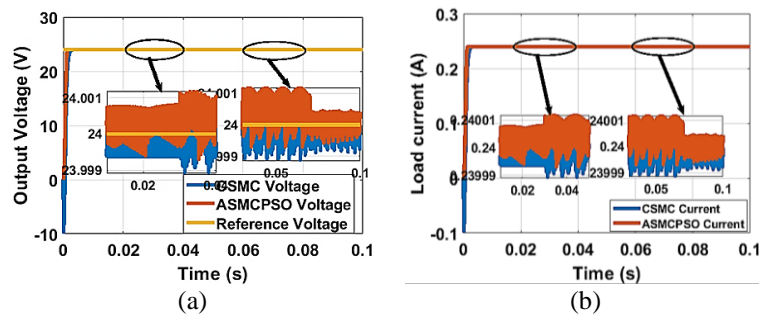


Figure 6. Comparing suggested controller simulation results with its conventional counterpart (2nd scenario): (a) output voltage and (b) load current

4.1.3. Variation of input voltage in buck mode (3rd scenario)

Figure 7 represents the step changes in the input voltage of the converter operating in buck mode, while Figures 8(a) and 8(b) depict the results obtained with the converter controls by the classical and the suggested controllers. As shown in Figures 8(a) and 8(b), the third scenario involves setting the reference voltage to 24 volts and 10 W CPL. However, the system is susceptible to abrupt changes in input voltage, which can range from 48 volts to 40 volts at $t = 0.03$ s and from 40 volts to 60 volts at $t = 0.07$ s. The results show the robustness of the two control strategies, as shown in Figure 8, with ASMCP SO surpassing the other control strategy in terms of performance stability and speed.

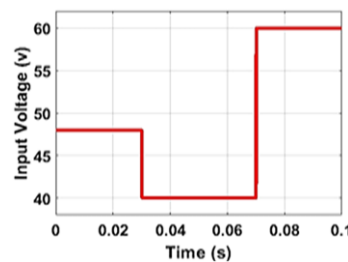


Figure 7. Step changes in the input voltage of the converter operating in buck mode

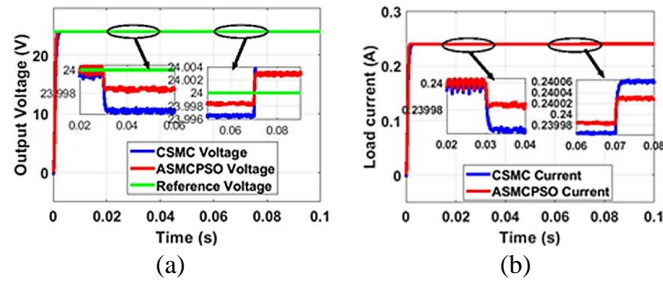


Figure 8. Comparing simulation results of the proposed controller with its conventional counterpart (2nd scenario): (a) output voltage and (b) load current

4.1.4. Variation of absorbed power in boost mode (4th scenario)

In the fourth scenario, the input and reference voltages are fixed, and the converter is now running in boost mode. The system is disrupted when the absorbed power changes suddenly from one value to another. The power changes from 10 watts to 5 watts at $t = 0.02$ seconds and from 5 watts to 20 watts at $t = 0.06$ seconds. The output voltage simulation results for the different control strategies are illustrated in Figure 9(a). Figure 9(b) represents the performance of all the control strategies, where the ASMCPSC performs better than the other controller when the load is adjusted.

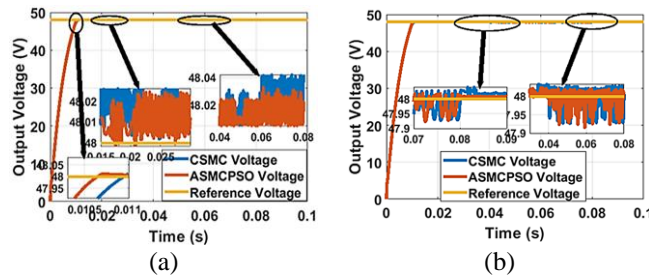


Figure 9. Comparing simulation results of proposed controller with its conventional counterpart: (a) variation of absorbed power (4th scenario) and (b) variation of input voltage (5th scenario)

4.1.5. Variation of input voltage in boost mode (5th scenario)

In the fifth scenario, the converter operates in boost mode, setting the output at 10 watts and the reference voltage at 48 volts. However, the system is susceptible to abrupt changes in input voltage, which occur at $t = 0.04$ and $t = 0.08$ seconds, respectively, going from 24 volts to 20 volts and 20 volts to 30 volts. ASMCPSC outperforms the other control technique in terms of performance stability and speed, as shown in Figure 9(b), which illustrates the robustness of the two control strategies. Tables 4 and 5 present a comparison of the results obtained from CSMC and ASMCPSC.

Table 4. Comparison of results obtained from CSMC and ASMCPSC in buck mod

| Simulations | $V_{in} = 48\text{ V}, V_{ref} = 24\text{ V}, P = 10\text{ W to } 20\text{ W at } 0.07\text{ s}$ | |
|--------------------|--|----------|
| Control strategy | CSMC | ASMCPSC |
| Settling time (ms) | 3.4 | 1.7 |
| Rise time (ms) | 1 | 0.9 |
| Overshoot (%) | 0 | 0 |
| IAE | 0.02714 | 0.01612 |
| ISE | 0.6208 | 0.2883 |
| SSE | 0.0003529 | 7.669e-5 |

Table 5. Comparison of results obtained from CSMC and ASMCPSC in boost mode

| Simulations | $V_{in} = 24\text{ V}, V_{ref} = 48\text{ V}, P = 10\text{ W to } 20\text{ W at } 0.03\text{ s}$ | |
|--------------------|--|---------|
| Control strategy | CSMC | ASMCPSC |
| Settling time (ms) | 10.9 | 10.5 |
| Rise time (ms) | 7.72 | 7.72 |
| Overshoot (%) | 0 | 0 |
| IAE | 0.183 | 0.1818 |
| ISE | 4.993 | 4.993 |
| SSE | 0.04115 | 0.00583 |

5. CONCLUSION

This study examined the instability of a two-way DC-DC converter with a resistive and CPL caused by negative incremental impedance. Conventional linear controllers are not able to stabilize such power

electronic devices. In order to stabilize a two-way DC-DC converter feeding a resistive and CPL, this work proposes an ASMC with a modified sliding surface based on particle swarm optimization. The ASMCPSO for stabilizing a bidirectional DC-DC converter feeding a resistive in parallel with a constant power demand has been validated by MATLAB/Simulink simulations. For additional validation of the suggested controller performance, simulation results under various reference voltage, input voltage, and absorbed power variations have been conducted. According to the observed results, DC microgrids can be stabilized by the ASMCPSO even in the presence of considerable changes in supply voltage and absorbed power. However, a PID or other conventional linear controller cannot provide this performance. The suggested controller will be put into practice later on to confirm the simulated outcomes. Furthermore, as distinct investigations are conducted in this work, a unified controller will be built to manage battery charging and discharging in DC microgrids.




REFERENCES

- [1] K. Louassaa, A. Chouder, and C. Rus-Casas, "Robust Nonsingular Terminal Sliding Mode Control of a Buck Converter Feeding a Constant Power Load," *Electron.*, vol. 12, no. 3, Feb. 2023, doi: 10.3390/electronics12030728.
- [2] Y. Yin, J. Mao, and R. Liu, "Multivariable-Feedback Sliding-Mode Control of Bidirectional DC/DC Converter in DC Microgrid for Improved Stability with Dynamic Constant Power Load," *Electron.*, vol. 11, no. 21, Nov. 2022, doi: 10.3390/electronics11213455.
- [3] S. Jaisudha, S. Srinivasan, and G. Kanimozhi, "Bidirectional resonant DC-DC converter for microgrid application," *International Journal of Power Electronics and Drive Systems*, vol. 8, no. 4, pp. 1548–1561, Dec. 2017, doi: 10.11591/ijpeds.v8i4.pp1548-1561.
- [4] D. Ochoa, S. Martinez, and P. Arévalo, "Extended Simplified Electro-Mechanical Model of a Variable-Speed Wind Turbine for Grid Integration Studies: Emulation and Validation on a Microgrid Lab," *Electron.*, vol. 11, no. 23, Dec. 2022, doi: 10.3390/electronics11233945.
- [5] Q. Xu, N. Vafamand, L. Chen, T. Dragicevic, L. Xie, and F. Blaabjerg, "Review on Advanced Control Technologies for Bidirectional DC/DC Converters in DC Microgrids," *IEEE Journal of Emerging and Selected Topics in Power Electronics*, vol. 9, no. 2, pp. 1205–1221, Apr. 2021, doi: 10.1109/JESTPE.2020.2978064.
- [6] J. Wu and Y. Lu, "Adaptive Backstepping Sliding Mode Control for Boost Converter With Constant Power Load," *IEEE Access*, vol. 7, pp. 50797–50807, 2019, doi: 10.1109/ACCESS.2019.2910936.
- [7] S. Neisarian, M. M. Arefi, N. Vafamand, M. Javadi, S. F. Santos, and J. P. S. Catalao, "Finite-time Adaptive Sliding Mode Control of DC Microgrids with Constant Power Load," in *2021 IEEE Madrid PowerTech, PowerTech 2021 - Conference Proceedings*, Institute of Electrical and Electronics Engineers Inc., Jun. 2021, doi: 10.1109/PowerTech46648.2021.9495071.
- [8] S. Singh, N. Rathore, and D. Fulwani, "Mitigation of negative impedance instabilities in a DC/DC buck–boost converter with composite load," *Journal of Power Electronics*, vol. 16, no. 3, pp. 1046–1055, May 2016, doi: 10.6113/JPE.2016.16.3.1046.
- [9] S. K. Ghosh, T. K. Roy, M. A. H. Pramanik, and M. A. Mahmud, "Design of nonlinear backstepping double-integral sliding mode controllers to stabilize the dc-bus voltage for dc–dc converters feeding cpls," *Energies*, vol. 14, no. 20, Oct. 2021, doi: 10.3390/en14206753.
- [10] Bharath K R, Harsha Choutapalli, P Kanakasabapathy, "Control of Bidirectional DC-DC Converter in Renewable based DC Microgrid with Improved Voltage Stability," *International Journal of Renewable Energy Research*, vol. 6, no.2, 2018, doi: 10.20508/ijrer.v8i2.7509.g7374.
- [11] M. H. Ashfaq, J. A. Selvaraj, and N. A. Rahim, "Control Strategies for Bidirectional DC-DC Converters: An Overview," *IOP Conference Series: Materials Science and Engineering*, vol. 1127, no. 1, p. 012031, Mar. 2021, doi: 10.1088/1757-899x/1127/1/012031.
- [12] A. Agarwal, K. Deekshitha, S. Singh, and D. Fulwani, "Sliding Mode Control of a Bidirectional DC/DC Converter with constant power load," in *IEEE International Conference on Engineering, Environmental Science*, 7 June 2015 doi: 10.1109/ICDCM.2015.7152056.
- [13] Nisha Kondrath, "An Overview of Bidirectional DC-DC Converter Topologies and Control Strategies for Interfacing Energy Storage Systems in Microgrids," *Journal of Electrical Engineering*, vol. 6, no. 1, Jan. 2018, doi: 10.17265/2328-2223/2018.01.002.
- [14] Y. Alidrisi, R. Ouladsine, A. Elmouatamid, R. Errouissi, and M. Bakhouya, "Constant Power Load Stabilization in DC Microgrids Using Continuous-Time Model Predictive Control," *Electron.*, vol. 11, no. 9, May 2022, doi: 10.3390/electronics11091481.
- [15] N. Tiwary, N. Venkatramana Naik, A. K. Panda, R. K. Lenka, and A. Narendra, "Super twisting sliding mode control of dual active bridge DC-DC converter," in *9th IEEE International Conference on Power Electronics, Drives and Energy Systems, PEDES 2020*, Institute of Electrical and Electronics Engineers Inc., Dec. 2020, doi: 10.1109/PEDES49360.2020.9379589.
- [16] M. Monsalve-Rueda, J. E. Candelo-Becerra, and F. E. Hoyos, "Second-Order Sliding-Mode Control Applied to Microgrids: DC & AC Buck Converters Powering Constant Power Loads," *Energies*, vol. 17, no. 11, Jun. 2024, doi: 10.3390/en17112701.
- [17] O. Kaplan and F. Bodur, "Super twisting algorithm based sliding mode controller for buck converter with constant power load," in *9th International Conference on Smart Grid, icSmartGrid 2021*, Institute of Electrical and Electronics Engineers Inc., Jun. 2021, pp. 137–142, doi: 10.1109/icSmartGrid52357.2021.9551244.
- [18] N. Janaki and R. K. Kumar, "A Comprehensive Review on Various Optimization Techniques for Zero Ripple Input Current DC-DC Converter," *International Journal of Pure and Applied Mathematics*, vol. 118, no. 5, pp. 39–49, 2018.
- [19] Agalya V and Sumathi S, "Optimization In Recent Aspects Of Power Converter," *International Journal of Scientific & Technology Research Volume*, vol. 8, no. 11, pp. 3756- 3762, 2019.
- [20] B. Wang, C. Wang, Q. Hu, G. Ma, and J. Zhou, "Adaptive sliding mode control with enhanced optimal reaching law for boost converter based hybrid power sources in electric vehicles," *Journal of Power Electronics*, vol. 19, no. 2, pp. 549–559, 2019, doi: 10.6113/JPE.2019.19.2.549.
- [21] H. Shi, H. Wen, Y. Hu, and L. Jiang, "Reactive Power Minimization in Bidirectional DC-DC Converters Using a Unified-Phasor-Based Particle Swarm Optimization," *IEEE Transactions on Power Electronics*, vol. 33, no. 12, pp. 10990–11006, Dec. 2018, doi: 10.1109/TPEL.2018.2811711.
- [22] G. Mustafa, F. Ahmad, R. Zhang, E. U. Haq, and M. Hussain, "Adaptive sliding mode control of buck converter feeding resistive and constant power load in DC microgrid," *Energy Reports*, vol. 9, pp. 1026–1035, Mar. 2023, doi: 10.1016/j.egy.2022.11.131.
- [23] Y. Cheddadi, Z. El Idrissi, F. Errahimi, and N. E. sbai, "Robust integral sliding mode controller design of a bidirectional DC charger in PV-EV charging station," *International Journal of Digital Signals and Smart Systems*, vol. 5, no. 2, p. 137, 2021, doi: 10.1504/ijdsss.2021.114557.




- [24] A.J.Mehta, and B.B.Naik, "Adaptive Sliding Mode Controller with Modified Sliding Function for DC-DC Boost Converter," in *IEEE International Conference on Power Electronics, Drives and Energy Systems (PEDES)*, December 2014, doi: 10.1109/PEDES.2014.7042009.
- [25] P. Nayana Menon, "A Practical Particle Swarm Optimized Sliding Mode Controller for an AC-DC Boost Converter," *International Journal of Scientific & Engineering Research*, vol. 5, no. 8, pp. 320- 325, 2014.
- [26] K. E. Fahim, M. S. Hossain, M. K. Afgani, S. M. Farabi, and S. Shajid, "Modelling and Simulation of DC-DC Boost Converter using Sliding Mode Control," *International Journal of Recent Technology and Engineering (IJRTE)*, vol. 9, no. 2, pp. 674–678, Jul. 2020, doi: 10.35940/ijrte.B3846.079220.
- [27] K. K. Mathew and D. M. Abraham, "PWM-Based Sliding Mode Current Controller for Bidirectional DC-DC Converters in Electric Vehicles," in *Proceedings of 2020 IEEE International Conference on Power, Instrumentation, Control and Computing, PICC 2020*, Institute of Electrical and Electronics Engineers Inc., Dec. 2020. doi: 10.1109/PICC51425.2020.9362431.

BIOGRAPHIES OF AUTHORS






Julius Derghe Cham    is a Ph.D. student in the Laboratory of Technology and Applied Science at the University of Douala. He received his DIPET II, M.Sc., and M.Eng. degrees in Electrical Engineering from the University of Bamenda, Douala, and Buea in 2015, 2020, and 2021, respectively. His research interests include the fields of power electronics, renewable energy, artificial intelligence, and non-linear control. He can be contacted at email: julius.cham@yahoo.com.






Francis Lénine Djanna Koffi    is an academic researcher at the University of Douala, specializing in Environmental Science and Biomass Ecology. With a strong record of scholarly contributions, he has participated in over 30 conferences and has authored more than 30 peer-reviewed scientific publications. He has also played a significant role in academic mentorship, supervising 30 master's and 5 Ph.D. thesis. Currently, he serves as the head of the Division of Internships, where he is responsible for overseeing permanent training and fostering relationships with professional skills networks. He can be contacted at email: djannaf@yahoo.com.



Alexandre Teplaira Boum    is full professor in Electrical Engineering. He holds of master degree in Electrical Engineering and a Ph.D. in Process Control. His domain of interest is process control, optimization, embedded systems, smart grid, and supervisory control. He can be contacted at email: boumat2002@yahoo.fr.



Ambe Harrison    is an independent researcher affiliated with the Department of Electrical and Electronics Engineering at the College of Technology (COT), University of Buea, Cameroon. His is currently interested in renewable energy development studies (Africa), real-time climatic resource estimation and optimization of PV systems, solar emulation, and nonlinear control. Harrison has authored/co-authored over 25 papers and reviewed more than 60 scientific articles. He is the founder of the Africa Renewable Energy Hub (AREH), an initiative dedicated to advancing renewable energy development in Africa through research and communication. He can be contacted at email: ambe.harrison@ubuea.cm.